


Cite this: *RSC Adv.*, 2017, 7, 25978

# Improved bioavailability of curcumin in liposomes prepared using a pH-driven, organic solvent-free, easily scalable process

Ce Cheng,<sup>a</sup> Shengfeng Peng,<sup>a</sup> Ziling Li,<sup>ab</sup> Liqiang Zou,<sup>a</sup> Wei Liu <sup>\*a</sup> and Chengmei Liu<sup>a</sup>

The poor water solubility and bioavailability of curcumin can be improved by encapsulating it into liposomes. However, the existing encapsulation technologies, such as the thin film method and the ethanol injection method, are complex and require the use of organic solvents. In this study, an organic solvent-free and easily scalable encapsulation technique was studied by utilizing the pH-dependent solubility properties of curcumin. Phospholipid was dissolved in water to form liposomes. Curcumin was deprotonated and dissolved under alkaline conditions and then encapsulated into the liposomes after acidification. Morphological observation and X-ray diffraction analysis confirmed that curcumin liposomes had been successfully prepared. Curcumin liposomes prepared by the pH-driven method were stable during storage. During *in vitro* digestion, curcumin liposomes prepared by the pH-driven method showed similar bioaccessibility to those prepared by the thin film method and higher bioaccessibility than those prepared by the ethanol injection method. The pH-driven method, which is organic solvent-free and easily scalable for industrial production, is thus a promising method for the preparation of curcumin liposomes.

Received 9th March 2017

Accepted 4th May 2017

DOI: 10.1039/c7ra02861j

rsc.li/rsc-advances

## 1. Introduction

Curcumin, a hydrophobic polyphenol, has a variety of potentially beneficial effects on human health, including antioxidant, anti-inflammatory, antimicrobial and anticarcinogenic activities.<sup>1,2</sup> These properties make curcumin suitable as a nutraceutical or pharmaceutical; however, the use of curcumin in food and pharmaceuticals is restricted by its poor water solubility, high susceptibility to degradation and low oral bioavailability.<sup>3</sup> To overcome these problems, curcumin has been incorporated into various carrier systems including nanoparticles,<sup>4</sup> emulsions,<sup>5</sup> halloysite particles,<sup>6–8</sup> capsules,<sup>9,10</sup> excipient emulsions,<sup>11–13</sup> and liposomes.<sup>14,15</sup>

Liposomes are self-assembled spherical vesicles with one or more concentric phospholipid bilayers that encapsulate a fraction of the surrounding aqueous medium.<sup>16</sup> Liposomes can transport both hydrophilic and hydrophobic components by entrapping them in the inner aqueous phase and incorporating them into the lipid bilayers, respectively.<sup>17</sup> Curcumin-loaded liposomes (CLs) have been prepared mainly by the thin film method<sup>15,18–22</sup> or the ethanol injection method,<sup>17</sup> and the

properties and stability of these CLs have been widely studied by a number of groups. Our group has also investigated CLs prepared by the thin film method<sup>14,23</sup> and ethanol injection method.<sup>24</sup> However, the organic solvents used in both these methods are unacceptable in food products. Recently, a novel, organic solvent-free encapsulation method, the pH-driven method, was developed.<sup>25,26</sup> This method is based on the deprotonation and dissolution of hydrophobic phytochemicals (such as curcumin and rutin) under alkaline conditions followed by neutralization to encapsulate the precipitated hydrophobic phytochemicals. To the best of our knowledge, the pH-driven method has not been utilized in the preparation of liposomes.

In this study, CLs were first prepared by a novel pH-driven method. We found that CLs could be produced by a pH-driven method that makes use of the self-assembly behavior of phospholipids in water together with the pH-dependent solubilization of curcumin. First, phospholipid was dissolved in water and self-assembled to form liposomes. The pH of the liposome solution was then increased to dissolve curcumin. Finally, curcumin was incorporated into the liposomes by acidifying the solution. To understand the procedure, the encapsulation efficiency, particle size and zeta potential of liposomes during the pH-driven process were determined. The encapsulation efficiency, particle size distribution and microstructure of the CLs formed by the pH-driven method (PDM-CLs) were then compared with those of CLs prepared using

<sup>a</sup>State Key Laboratory of Food Science and Technology, Nanchang University, Nanchang 330047, Jiangxi, PR China. E-mail: liuweili@ncu.edu.cn; Fax: +86 791 88334509; Tel: +86 791 88305872 ext. 8106

<sup>b</sup>School of Life Science, Jiangxi Science and Technology Normal University, Nanchang, 330013, Jiangxi, PR China



the thin film method (TFM-CLs) and the ethanol injection method (EIM-CLs). The stabilities of the PDM-CLs, TFM-CLs and EIM-CLs after treatment with sodium chloride and after storage were also evaluated. Finally, the bioaccessibility of curcumin was evaluated using a simulated gastrointestinal tract.

## 2. Experimental

### 2.1 Materials

Curcumin (98%) was purchased from Aladdin Industrial Corporation (Shanghai China). Phospholipid [Lipoid S75, consisting mainly of phosphatidylcholine (70%), phosphatidylethanolamine (10%) and lysophosphatidylcholine (2%)] was obtained from Lipoid GmbH (Ludwigshafen, Germany). Mucin from porcine stomach and Nile red were obtained from Sigma-Aldrich Chemical Co. (St. Louis, MO, USA). Ethanol and other reagents were all of analytical grade.

### 2.2 Preparation protocol

CLs were prepared by the pH-driven method, the thin film method and the ethanol injection method. The phospholipid concentration was  $10 \text{ mg mL}^{-1}$ , and the curcumin feed concentration was  $0.4 \text{ mg mL}^{-1}$ . The obtained CLs were filtrated through filter paper to remove any crystalline curcumin.

**2.2.1 pH-driven method.** PDM-CLs were prepared using the method described by Pan *et al.*<sup>25</sup> with minor modifications. Curcumin and phospholipid were added to super-pure water and stirred for at least 4 h at room temperature. The pH of the solution was then adjusted to 12.0 with 4 M NaOH. After stirring for 20 min, the pH of the solution was adjusted back to 5.3 with 4 M HCl, and the PDM-CLs were collected.

**2.2.2 Thin film method.** TFM-CLs were produced as described in our previous study.<sup>14</sup> Briefly, phospholipid and curcumin were dissolved in absolute ethanol, and the ethanol was then evaporated using a rotary evaporator. The resulting thin film was hydrated with super-pure water for 30 min, and the TFM-CLs were collected.

**2.2.3 Ethanol injection method.** EIM-CLs were formed as described in our previous study.<sup>24</sup> Briefly, phospholipid and curcumin were dissolved in absolute ethanol. The ethanol solution was dropped into super-pure water and stirred for 30 min. The TFM-CLs were collected after the evaporation of residual ethanol using a rotary evaporator.

### 2.3 Characterization of PDM-CLs

**2.3.1 Degradation of curcumin.** The degradation of curcumin at pH 12.0 was studied. Briefly, curcumin stock solution ( $5 \text{ mg mL}^{-1}$  in methanol,  $300 \mu\text{L}$ ) was dissolved in phospholipid solution ( $0.5 \text{ mg mL}^{-1}$ ,  $50 \text{ mL}$ ), and the combined solution was adjusted to pH 12.0 using 4 M NaOH. The absorbance spectra of curcumin were obtained from 350 to 700 nm at 5 min intervals using an ultraviolet-visible (UV-Vis) spectrometer (Pgeneral T6, China) with phospholipid solution as the blank.

**2.3.2 Liposome morphology.** The morphologies of the liposomes after hydration in water were confirmed by confocal

laser scanning microscopy using Nile red fluorescent lipid label. To stain the liposomal membrane, Nile red in methanol ( $1 \text{ mg mL}^{-1}$ ,  $40 \mu\text{L}$ ) was added to the solution of liposomes ( $1 \text{ mL}$ ). The samples were then observed using a LSM710 confocal laser scanning microscope (Zeiss, Germany).

**2.3.3 Encapsulation efficiency (EE).** The CLs were centrifuged at  $8000 \text{ g}$  for 10 min under acidic conditions using an OPTIMA MAX-XP ultracentrifuge (Beckman Coulter, Fullerton, CA, USA) to remove the unencapsulated curcumin. The supernatant (containing loaded curcumin) was removed and diluted with anhydrous ethanol. Absorbance at 420 nm was measured using a UV-Vis spectrometer, and the concentration of loaded curcumin was calculated from the calibration curve. EE was then calculated from the UV-Vis data using eqn (1). When the curcumin was dissolved under alkaline conditions, the CLs were separated from unencapsulated curcumin by centrifugation at  $650\,000 \text{ g}$  for 30 min. The concentration of free curcumin (supernatant) was determined by UV-Vis spectrophotometry, and EE was then calculated according to eqn (1):

$$\text{EE (\%)} = \frac{\text{loaded curcumin}}{\text{initial curcumin}} \times 100. \quad (1)$$

**2.3.4 Particle size and zeta potential.** To further understand the pH-driven method, the particle size and zeta potential of the liposomes were measured at pH 5.3 (after alkalization to pH 12.0 and subsequent acidification to pH 5.3) using a Zetasizer Nano ZS instrument (Malvern Instruments Ltd, Malvern, UK). The raw data were subsequently converted to mean hydrodynamic size by cumulant analysis. The intensity was detected at an angle of  $90^\circ$ . The dispersions were diluted 20 times using super-pure water or super-pure water previously adjusted to pH 12.0 using 4 M NaOH. All data presented are the averages of at least triplicate measurements.

**2.3.5 Microstructure.** The microstructures of the PDM-CLs, TFM-CLs and EIM-CLs were studied using transmission electron microscopy. Briefly, a copper mesh grid was placed onto droplets of sample solution diluted to a phospholipid concentration of  $1 \text{ mg mL}^{-1}$  with super-pure water. After 3 min, the grid was stained with phosphotungstic acid solution (1%) for 4 min and air-dried at room temperature after removing the excess liquid with filter paper. The grid containing the samples was examined under a JEM-2100 transmission electron microscope (JEOL, Ltd., Tokyo, Japan) at a voltage of 200 kV.

**2.3.6 X-ray powder diffraction (XRD).** The XRD patterns of crystalline curcumin and the PDM-CLs, TFM-CLs and EIM-CLs were recorded using a D8 Advance X-ray diffractometer (Bruker, Germany). The divergence slit was set at  $1^\circ$ , and the receiving slit was set at 0.1 mm for the incident beam. The scan rate was  $2^\circ$  per min over a  $2\theta$  angle range of  $5^\circ$ – $60^\circ$ .

### 2.4 Stability study

**2.4.1 Salt stability.** The influence of ionic strength on the stabilities of the PDM-CLs, TFM-CLs and EIM-CLs was determined by treatment with aqueous NaCl solution (10, 50, 100, 200, 500, and 1000 mM) for 1 h at room temperature. The size distributions of the samples were determined, and the samples



were photographed using a digital camera after storage for 1 h and 3 d at 4 °C.

**2.4.2 Storage stability.** To evaluate shelf life, the PDM-CLs, TFM-CLs and EIM-CLs were stored in a container at 4 °C in the dark. Changes in the size distributions and EE values were investigated every three days during storage for one month.

## 2.5 Simulated gastrointestinal digestion

The potential gastrointestinal fates of the PDM-CLs, TFM-CLs and EIM-CLs were analyzed by passing them through a simulated gastrointestinal tract consisting of mouth, stomach, and small intestine phases, as described in our previous report but with minor modifications.<sup>11</sup>

**2.5.1 Mouth phase.** A simulated saliva fluid containing mucin (30 mg mL<sup>-1</sup>) along with various salts was prepared as described elsewhere.<sup>27</sup> Each sample (3 mL) was mixed with simulated saliva fluid (3 mL) preheated to 37 °C. The pH of the resulting mixture was then adjusted to 6.8 with 50 mM NaOH. The mixtures were shaken at 90 rpm for 10 min at 37 °C to mimic oral conditions.

**2.5.2 Gastric stage.** Simulated gastric fluid was prepared by adding NaCl (2 g) and HCl (7 mL) to 1 L of super-pure water. Simulated gastric fluid (6 mL) containing pepsin (3.2 mg mL<sup>-1</sup>) was preheated to 37 °C and added to the sample from the mouth phase. The mixtures were then adjusted to pH 2.5 and shaken at 100 rpm for 2 h to mimic digestion in the stomach.

**2.5.3 Small intestine phase.** Samples from the simulated gastric model were diluted with phosphate-buffered saline (10 mM, 12 mL, pH 6.5). The diluted mixtures were shaken at 37 °C for 10 min, and the solutions were then adjusted to pH 7.0. Simulated small intestinal fluid containing pancreatin (24 mg mL<sup>-1</sup>, 2 mL), bile extract solution (50 mg mL<sup>-1</sup>, 2.8 mL) and saline solution (0.5 M CaCl<sub>2</sub> and 7.5 M NaCl, 1.2 mL) were added into the digestion samples. The pH of each digestion sample was maintained at pH 7.0 by the addition of 50 mM NaOH.

**2.5.4 Curcumin concentration and bioaccessibility after digestion.** After *in vitro* digestion, the raw digesta in each mixture was centrifuged at 40 000g for 30 min at 4 °C. The supernatants were collected and assumed to be micellar fractions in which the bioactive compound is solubilized. The solubilized curcumin was diluted with methanol and assayed using a 1260 HPLC system (Agilent Technologies, Santa Clara, CA, USA) equipped with a UV-Vis detector. Curcumin was separated on a Sunfire C 18 column (250 mm × 4.6 mm, 5 μm; Waters Corporation, Milford, MA, USA), using a mobile phase consisting of 0.1% (v/v) acetic acid and acetonitrile (45 : 55 v/v) at a flow rate of 1.0 mL min<sup>-1</sup>. Detection was achieved by UV absorption at 420 nm.

The transformation, bioaccessibility and micellization of the curcumin were then calculated using the following respective equations:

$$\text{Transformation (\%)} = C_{\text{Digesta}}/C_{\text{Initial}} \times 100 \quad (2)$$

and

$$\text{Bioaccessibility (\%)} = C_{\text{Micelles}}/C_{\text{Digesta}} \times 100, \quad (3)$$

where  $C_{\text{Micelles}}$  and  $C_{\text{Digesta}}$  are the concentrations of curcumin in the mixed micelle fraction and in the overall digesta after the simulated digestion, respectively, and  $C_{\text{Initial}}$  is the concentration of added curcumin.

## 2.6 Statistical analysis

All measurements were replicated at least three times. The results are expressed as means ± standard deviations. Data were subjected to statistical analysis using SPSS software, version 18.0 (SPSS Inc., Chicago, IL, USA). The Student–Newman–Keuls test was performed to determine significance, and  $P < 0.05$  was considered statistically significant.

# 3. Results and discussion

## 3.1 Preparation and characterization of PDM-CLs

The process for preparing the PDM-CLs is depicted in Fig. 1A. First, weighed amounts of curcumin and phospholipid were added to super-pure water (Fig. 1AI). After agitation for 4 h, the phospholipid was fully dissolved and had self-assembled into liposomes with an average diameter of 980.5 nm and a zeta potential of −53.7 mV (Fig. 1AII). Confocal laser scanning microscopy showed that the liposomes were smooth spherical vesicles with particle sizes in the range of 500–1500 nm. The EE of curcumin into the liposomes was 14.1% ± 1.6%, indicating that liposomes had been prepared by dissolving the phospholipid in water, and that curcumin was loaded into liposomes, but with low EE. The liposome solution was then adjusted to pH 12.0 using 4 M NaOH to dissolve curcumin (Fig. 1AIII). The average diameter of the liposomes decreased from 980.5 to 220.3 nm, and the zeta potential decreased from −53.7 to −91.9 mV when the pH was increased to 12.0 (Fig. 1C). Under alkaline conditions, the amount of curcumin loaded into the liposomes also decreased from 14.1% ± 1.6% to 3.0% ± 0.5%. At pH 12.0, deprotonated curcumin become unstable, deep red in color, and water soluble.<sup>28</sup> This observation prompted us to examine the stability of curcumin with liposomes at pH 12.0. The visible light spectrum of curcumin during incubation in alkaline solution (pH 12.0) for 60 min is shown in Fig. 1B. The reduction in absorbance at 468 nm ( $\text{Abs}_{468}$ ) was used to indicate the possible degradation of curcumin under alkaline conditions.<sup>29</sup> At pH 12.0, the  $\text{Abs}_{468}$  of curcumin decreased by 1.2% after incubation for 20 min and by 3.8% after incubation for 60 min. In contrast, the  $\text{Abs}_{468}$  of curcumin at pH 12.0 without additives decreased by 5.8% after 60 min. Similarly, another study indicated that the  $\text{Abs}_{468}$  of curcumin at pH 12.0 without additives and in the presence of sodium casein were decreased by 4.3% and 2.9%, respectively.<sup>25</sup> In the present study, the curcumin was completely dissolved after 20 min, indicating that decomposition was negligible, and that CLs could be safely prepared at pH 12.0. After 20 min, the pH of the solution was adjusted back to 5.3 with 4 M HCl (Fig. 1AIV), and the PDM-CLs were collected. The EE, average diameter, polydispersity index and zeta potential of the PDM-CLs were 62.8% ± 1.4%, 217.5 nm, 0.248 and −53.1 mV, respectively. A transmission electron microscopy image (Fig. 1AIV) showed that the PDM-



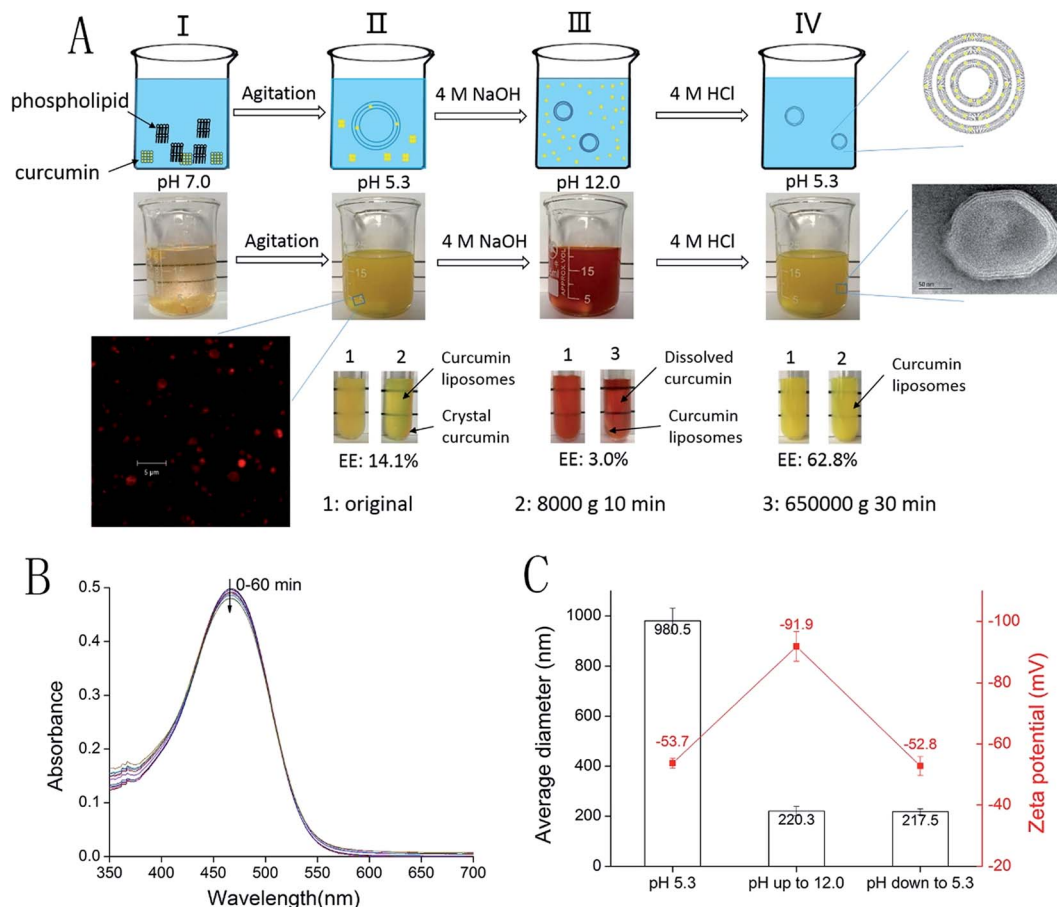


**Fig. 1** (A) Schematic and photographs of the pH-driven process along with a picture showing the determination of encapsulation efficiency. (B) Absorbance spectra of curcumin dissolved in aqueous solutions at pH 12.0; the spectra were collected every 5 min for up to 60 min at 20 °C. (C) Changes in the particles size and zeta potential of liposomes during the pH-driven process.

CLs were spherical, multilamellar vesicles. The CLs could thus be successfully prepared using the pH-driven method, with no need for organic solvents or specific equipment. The process is simple, easy to control, and suitable for industrial production.

There are two noteworthy phenomena associated with the pH-driven process. First, the particle size of the liposomes dramatically decreased from 980.5 to 220.3 nm after alkalization to pH 12.0. This reduction in diameter could be caused by the osmotic force generated by the ionic gradient across the membrane, leading to the evacuation of water from the inner core of the liposome.<sup>30</sup> On the other hand, because the zeta potential decreased from -53.7 to -91.9 mV when the pH increased to 12.0, we speculated that increased repulsive electrostatic forces changed the curvature of the bilayer and decreased the particle size. Second, the EE of the CLs decreased from 14.1% to 3.0% when the pH increased from 5.3 to 12.0 and increased from 3.0% to 62.8% when the pH decreased from 12.0 to 5.3 (Fig. 1A). Curcumin is insoluble (hydrophobic form) at pH 5.3 and soluble (hydrophilic form) at pH 12.0. At lower pH, the diffusion of the hydrophobic form of curcumin into liposomal membranes is likely driven by hydrophobic forces. In the pH-driven process, the EE of the CLs increased from 14.1% to 62.8%. This phenomenon can be explained by the different

states of curcumin. When curcumin and phospholipid are mixed in water at low pH, the hydrophobic form of curcumin is not in contact with the liposomal membrane, resulting in a very low EE. During the pH-driven process, curcumin was dissolved in water at pH 12.0 and made full contact with the liposomal

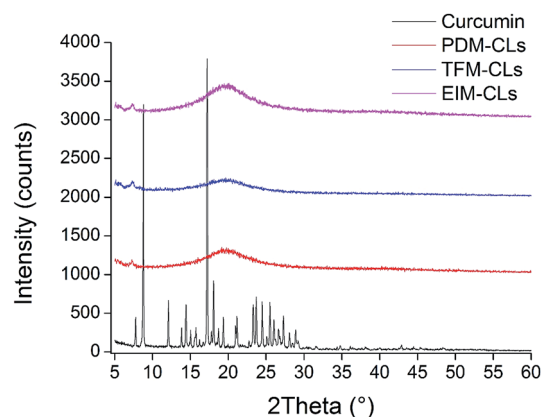


**Fig. 2** XRD spectra of curcumin liposomes produced by the pH-driven method (PDM-CLs), thin film method (TFM-CLs) and ethanol injection method (EIM-CLs).





**Table 1** Average diameter, polydispersity index, zeta potential, initial added curcumin concentration ( $C_{\text{Initial}}$ ), total curcumin concentration after digestion ( $C_{\text{Digesta}}$ ), curcumin concentration in micelles after digestion ( $C_{\text{Micelles}}$ ), transformation and bioaccessibility of curcumin liposomes produced by the pH-driven method (PDM-CLs), thin film method (TFM-CLs) and ethanol injection method (EIM-CLs). Statistical analysis: different letters (a, b) in the same row for each parameter are significantly different (SNK test,  $P < 0.05$ )

	PDM-CLs	TFM-CLs	EIM-CLs
Average diameter (nm)	217.5 $\pm$ 11.7 <sup>b</sup>	453.3 $\pm$ 86.0 <sup>a</sup>	115.1 $\pm$ 3.4 <sup>c</sup>
Polydispersity index	0.248 $\pm$ 0.027 <sup>b</sup>	0.531 $\pm$ 0.059 <sup>a</sup>	0.243 $\pm$ 0.046 <sup>b</sup>
Zeta potential (mV)	−53.1 $\pm$ 3.3 <sup>a</sup>	−54.0 $\pm$ 2.9 <sup>a</sup>	−52.9 $\pm$ 3.5 <sup>a</sup>
$C_{\text{Initial}}$ ( $\mu\text{g mL}^{-1}$ )	401.3 $\pm$ 7.8 <sup>a</sup>	402.3 $\pm$ 8.7 <sup>a</sup>	177.7 $\pm$ 7.8 <sup>b</sup>
$C_{\text{Digesta}}$ ( $\mu\text{g mL}^{-1}$ )	176.7 $\pm$ 10.0 <sup>a</sup>	173.7 $\pm$ 14.1 <sup>a</sup>	79.0 $\pm$ 14.2 <sup>b</sup>
$C_{\text{Micelles}}$ ( $\mu\text{g mL}^{-1}$ )	95.2 $\pm$ 1.3 <sup>a</sup>	95.8 $\pm$ 4.0 <sup>a</sup>	36.8 $\pm$ 3.4 <sup>b</sup>
Transformation (%)	44.2 $\pm$ 2.5 <sup>a</sup>	43.4 $\pm$ 3.5 <sup>a</sup>	41.5 $\pm$ 1.7 <sup>a</sup>
Bioaccessibility (%)	54.1 $\pm$ 3.7 <sup>a</sup>	55.4 $\pm$ 2.4 <sup>a</sup>	48.5 $\pm$ 3.3 <sup>b</sup>

membrane. When the pH decreased to 5.3, the curcumin was transformed from the hydrophilic form to the hydrophobic form and diffused into the liposomal membrane driven by hydrophobic forces. According to the report of Khoury *et al.*,<sup>31</sup> the partition coefficient of curcumin in liposomes is remarkable, with partition coefficients of  $2.78 \times 10^5$  in the solid gel phase and  $1.15 \times 10^6$  in the liquid crystalline phase. A high

partition coefficient encourages membrane permeability; thus, the incorporation of curcumin into the membrane is remarkable. Therefore, the pH-driven method was a suitable candidate to prepare CLs.

To evaluate the crystallinity of curcumin in liposomes, curcumin, PDM-CLs, TFM-CLs and EIM-CLs were analyzed by XRD (Fig. 2). The diffraction pattern of curcumin showed peaks at  $2\theta = 8.79^\circ$ ,  $12.09^\circ$ ,  $14.42^\circ$ ,  $17.22^\circ$ , and  $24.50^\circ$ , indicating a highly crystalline structure.<sup>32</sup> On the other hand, none of the CLs showed obvious diffraction peaks, indicating that curcumin exists in an amorphous rather than crystalline state in the liposomes.

The average diameter of the EIM-CLs was 115.1 nm, with a polydispersity index of 0.245; the corresponding values for the TFM-CLs were 453.3 nm and 0.531, respectively. The average diameter of the PDM-CLs was thus smaller than that of the TFM-CLs but higher than that of the EIM-CLs. The polydispersity index of the PDM-CLs was similar to that of the EIM-CLs and significantly smaller than that of the TFM-CLs, indicating a narrower size distribution. The zeta potential of the PDM-CLs (−53.1 mV) was not significantly different ( $P > 0.05$ ) from that of the TFM-CLs (−54.0 mV) or EIM-CLs (−52.9 mV).

The EEs of the PDM-CLs, TFM-CLs and EIM-LPs were  $62.8\% \pm 1.4\%$ ,  $78.6\% \pm 2.3\%$  and  $46.6\% \pm 1.0\%$ , respectively. EE values in the range of 45–97.8% have been reported for CLs prepared using different methods, phospholipid compositions and curcumin-to-phospholipid ratios.<sup>15,17,20,22,33,34</sup> The EE of the

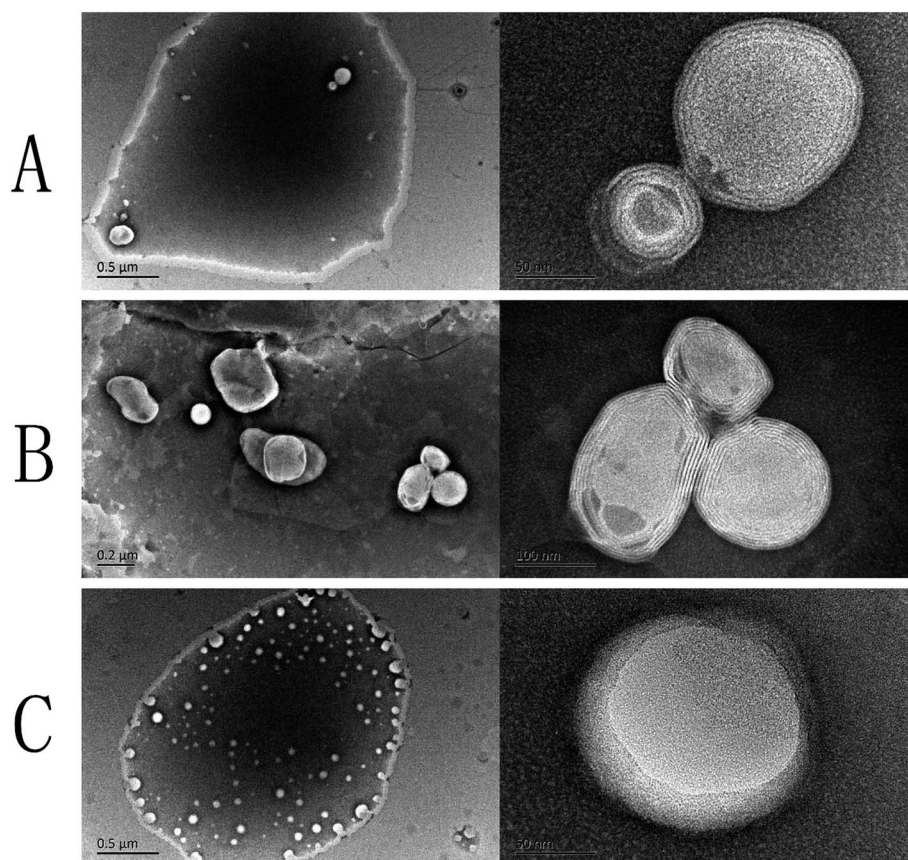


**Fig. 3** Transmission electron microscopy images of curcumin liposomes produced by the (A) pH-driven method, (B) thin film method, and (C) ethanol injection method.



PDM-CLs was  $\sim 16\%$  higher than that of the EIM-LPs but  $\sim 16\%$  lower than that of the TFM-CLs. The total curcumin concentrations (after filtration through filter paper to remove crystalline curcumin) of the PDM-CLs, TFM-CLs and EIM-LPs were 0.401, 0.402, and 0.177 mg mL<sup>-1</sup>, respectively (Table 1). The total curcumin concentrations of the PDM-CLs and TFM-CLs were almost equal to the initial added curcumin concentration, indicating that the free curcumin in the PDM-CLs and TFM-CLs was soluble and retained in the liposomal dispersion after filtration. However, the total curcumin concentration of the EIM-CLs was equal to the amount of encapsulated curcumin, indicating that the free curcumin in EIM-CLs was crystalline and had been removed by filtration.

The structures of the PDM-CLs, TFM-CLs and EIM-LPs were confirmed by transmission electron microscopy (Fig. 3). The particle sizes of TFM-CLs, EIM-CLs and PDM-CLs were in the range 120–480 nm, 50–100 nm and 100–200 nm, respectively, in agreement with the data obtained by dynamic laser light scattering. Liposomes can be classified as either multilamellar vesicles or unilamellar vesicles depending on the number of bilayers. The transmission electron microscopy images showed that the PDM-CLs and TFM-CLs had spherical, multilamellar membrane structures, whereas the EIM-CLs were spherical, unilamellar vesicles. In the traditional thin film method, the dry phospholipid film of stacked bilayers is rehydrated under hydrodynamic flow, typically forming multilamellar vesicles.<sup>19,35</sup> During the ethanol injection method, the ethanol is diluted by the aqueous phase, and phospholipid molecules form bilayer fragments that assemble into unilamellar vesicles.<sup>35</sup> However, some studies have shown that liposomes prepared by the ethanol injection method have multilamellar structures.<sup>36,37</sup> This is the first study to establish that PDM-CLs have multilamellar structures. In the pH-driven method, phospholipid is dissolved in water and self-assembles into liposomes. Since there is no ethanol present, the phospholipid molecules do not form bilayer fragments; thus, the liposomes prepared by the pH-driven method are more likely to assemble into multilamellar vesicles.

### 3.2 Stability of PDM-CLs

The mean particle size and EE of the CLs were examined after storage for 1 month at 4 °C (Fig. 4). The TFM-CLs were unstable during storage and showed particle swelling and leakage of curcumin. After 30 days, the amount of curcumin encapsulated by the TFM-CLs decreased from 78.6% to 50.1%, and the particle size increased from 402.5 to 1650.3 nm. The PDM-CLs and EIM-CLs were relatively stable during storage. The amount of curcumin encapsulated by the PDM-CLs decreased from 66.0% to 64.8%, and the particle size of the PDM-CLs increased from 217.5 to 235.1 nm after 30 days at 4 °C. The amount of curcumin encapsulated by the EIM-CLs decreased from 38.9% to 36.9%, and the particle size of the EIM-CLs increased from 116.1 to 153.1 nm after 30 days at 4 °C. These results indicate that PDM-CLs are stable during storage at 4 °C, with little leakage of curcumin.

The influence of ionic strength on the stability of the PDM-CLs, TFM-CLs and EIM-CLs was evaluated by measuring

changes in particle size after incubation with different concentrations of NaCl (Fig. 5B). Although NaCl is produced during the preparation of PDM-CLs, the relatively low concentration present ( $\sim 20$  mM) did not influence the results of the stability study. The average diameter of the PDM-CLs increased gradually from 211 to 251 nm as the concentration of NaCl was increased to 1 M, whereas the average diameter of the EIM-CLs decreased gradually from 119.3 to 102.9 nm. The average diameter of the TFM-CLs first decreased from 400 to 300 nm and then increased markedly to 750 nm as the concentration of NaCl was gradually increased to 1 M. To further evaluate the stability of the CLs in solutions of different ionic strength, all samples were stored at 4 °C for 3 days and then visually examined (Fig. 5A). The transparency of the PDM-CLs decreased after treatment with 0.5 and 1 M NaCl, and some precipitation was observed. The TFM-CLs, however, only become turbid after treatment with high concentrations of NaCl ( $>200$  mM), and precipitation was observed only at concentrations  $>500$  mM. Changes in the appearance of the EIM-CLs were negligible

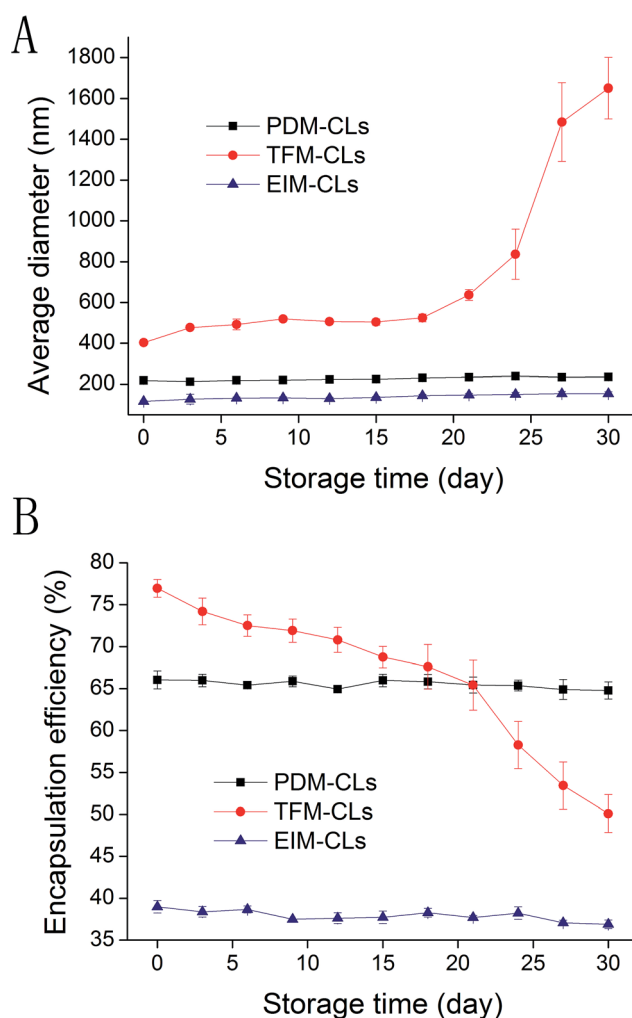


Fig. 4 Changes in average diameter (A) and encapsulation efficiency (B) of curcumin liposomes produced by the pH-driven method (PDM-CLs), thin film method (TFM-CLs) and ethanol injection method (EIM-CLs) during storage at 4 °C for one month.

following storage for 3 days in NaCl solutions of any ionic strength. These results indicate that TFM-CLs are sensitive to changes in ionic strength, whereas EIM-CLs are stable in a 1 M solution of NaCl. PDM-CLs have intermediate stability; they are stable at low concentrations of NaCl (<0.2 M) but less stable at higher concentrations of NaCl (>0.5 M).

The sizes of the EIM-CLs and TFM-CLs were found to decrease after treatment with NaCl solution, in agreement with earlier reports from us and others.<sup>23,30,38</sup> When the ionic gradient across the liposomal membrane is too high, an osmotic force is generated, and water flows out of the liposome to compensate for the high external ion concentration.<sup>39</sup> This causes a reduction in particle size until the maximum compaction of the bilayer is reached. This phenomenon was not observed in the PDM-CLs because it had already occurred during liposome formation (Fig. 1C). Liposomal dispersions are thermodynamically unstable. Because of attractive van der Waals forces, the total free energy of a dispersed system can be lowered by reducing the interfacial area.<sup>30</sup> According to the extended Derjaguin–Landau–

Verwey–Overbeek theory, there are two main repulsive forces, the electrostatic force and hydration force.<sup>30,40</sup> At relatively low NaCl concentration (<200 mM), the electrostatic and hydration forces were sufficiently strong to overcome the attractive force, and all three liposomal formulations were stable. At relatively high NaCl concentration (>500 mM), the counter-ions in NaCl screen the electrostatic repulsive forces acting between the particles.<sup>38</sup> In this situation, the stability of liposomes decreases in the order of EIM-CLs > PDM-CLs > TFM-CLs and is negatively correlated with particle size. This phenomenon can be attributed to the size-dependence of van der Waals forces. The van der Waals force between colloidal particles of radii  $R_1$  and  $R_2$  is expressed by the following equation:<sup>41</sup>

$$\text{van der Waals force} = -\frac{A}{6(r - R_1 - R_2)} \frac{R_1 R_2}{(R_1 + R_2)}, \quad (4)$$

where  $A$  is the Hamaker constant, and  $r$  is the distance between particle centers. From this equation, we find that the attractive van der Waals forces are positively correlated with the radii of the

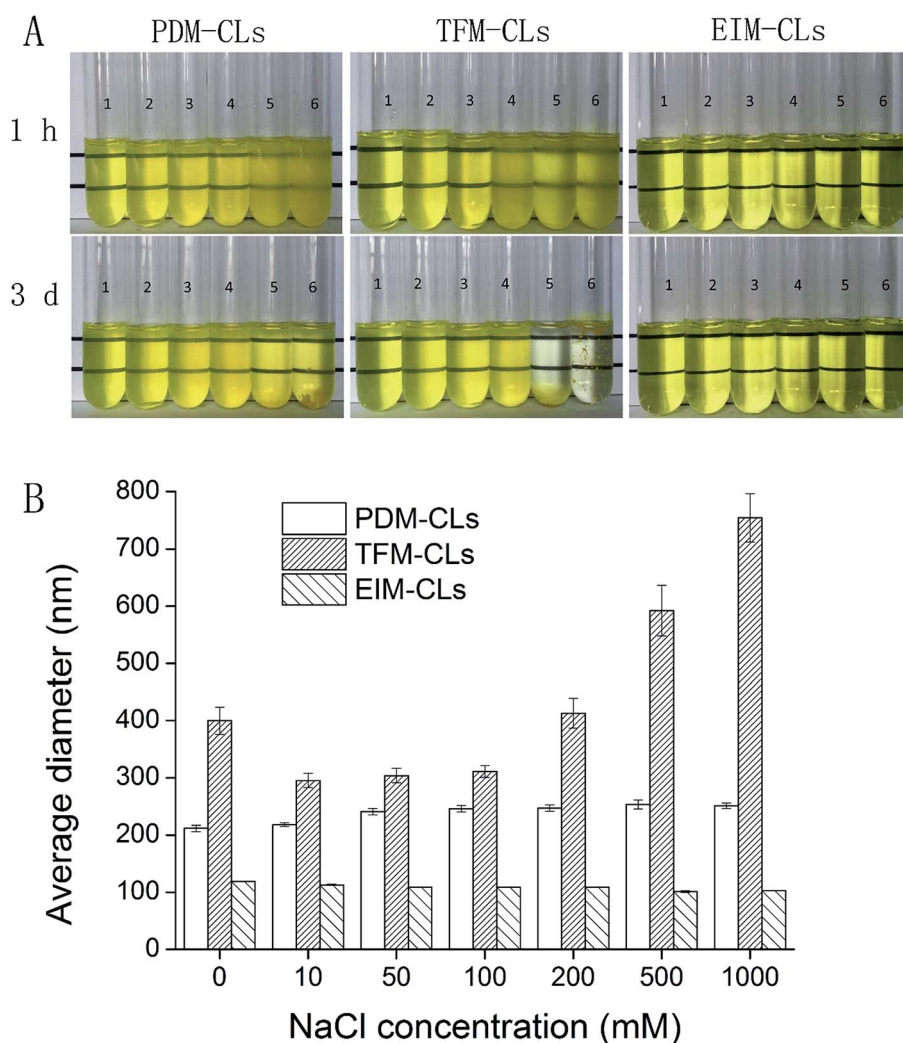


Fig. 5 Effect of NaCl concentration on the appearance after 1 hour and 3 days (A) and average diameters (B) of curcumin liposomes produced by the pH-driven method (PDM-CLs), thin film method (TFM-CLs) and ethanol injection method (EIM-CLs). 1–6 are the concentrations of NaCl (0, 50, 100, 200, 500 and 1000 mM, respectively).





colloidal particles. The smaller the liposomal particle size, the smaller the attractive van der Waals force, ultimately resulting in better stability. This phenomenon accounts for the negative correlation between the stability of EIM-CLs, PDM-CLs and TFM-CLs and particle size. On the other hand, the poor storage and ionic stability of the TFM-CLs might be due to the higher loaded amount of curcumin. Pérez-Lara *et al.* reported that curcumin disorders 1,2-dipalmitoyl-*sn*-glycero-3-phosphocholine membranes.<sup>42</sup> Barry *et al.* found that curcumin induces segmental ordering of the lipid membrane at low concentrations but disorders the acyl chain region of the lipid membrane at high concentrations.<sup>43</sup> In this study, the loaded curcumin concentration of the TFM-CLs was significantly higher than those of the EIM-CLs and PDM-CLs, which might also contribute to the instability of the TFM-CLs.

### 3.3 Curcumin bioaccessibility and degree of micellization of PDM-CLs

The influence of the preparation method on the transformation and bioaccessibility of curcumin was investigated using a simulated gastrointestinal tract (Table 1). The levels of transformation of the PDM-CLs, TFM-CLs and EIM-CLs were 44.2%, 43.4% and 41.5%, respectively, and were not significantly different ( $P > 0.05$ ). The transformation of a bioactive compound determines the amount of the compound that remains in a bioactive form. Curcumin degradation is caused by exposure to neutral or alkaline aqueous environments; thus, transformation is mainly reduced by preventing curcumin from coming into contact with the surrounding aqueous phase. In the present study, the digestion conditions were exactly the same, indicating that the PDM-CLs, TFM-CLs and EIM-CLs all protect curcumin to a similar extent.

The bioaccessibility is the fraction of the bioactive form that is available for absorption. The term bioaccessibility is a key concept for determining the nutritional efficiency of food and food formulas developed with the aim of improving human health.<sup>44</sup> *In vitro* methods have been developed to simulate physiologic conditions and the sequence of events that occur during digestion in the human gastrointestinal tract. In a recent study, we used a simulated gastrointestinal tract to compare the bioaccessibilities of CLs with curcumin-loaded zein nanoparticles and curcumin-loaded nanoemulsions.<sup>24</sup> However, there are no reports describing the influence of the preparation method on the bioaccessibility of CLs. In the present study, we found that the bioaccessibility of the PDM-CLs (54.1%) was similar to that of the TFM-CLs (55.4%) and significantly ( $P < 0.05$ ) higher than that of the EIM-CLs (48.5%). The bioaccessibility of curcumin in EIM-CLs was lower than those of curcumin in PDM-CLs and TFM-CLs, indicating that the preparation method affects liposomal bioaccessibility.

The amount of curcumin in the mixed micelle phase after simulated digestion can be assumed to be the part available for absorption. The micellization of curcumin from PDM-CLs ( $95.2 \mu\text{g mL}^{-1}$ ) was similar to that from TFM-CLs ( $95.8 \mu\text{g mL}^{-1}$ ) and significantly higher than that from EIM-CLs ( $36.8 \mu\text{g mL}^{-1}$ ). This result was attributed to the lower initial curcumin

concentration before simulated digestion since the free curcumin was crystalline and had been removed by filtration (as described in Section 3.1). The bioavailability of curcumin in the PDM-CLs was thus similar to that in the TFM-CLs and significantly higher than that in the EIM-CLs.

## 4. Conclusions

A pH-driven method had been successfully applied to prepare CLs. The method is based on the self-assembly behavior of phospholipid in water and the diffusion of curcumin into liposomal membranes driven by hydrophobic forces. The CLs prepared by the thin film method displayed high bioaccessibility but poor storage stability, and those prepared by the ethanol injection method were stable during storage but showed low bioaccessibility. The CLs prepared using the new pH-driven method showed high bioaccessibility and were stable during storage. The pH-driven method is a promising method to prepare CLs since it does not require organic solvents and is easily scalable for industrial production.

## Acknowledgements

We appreciate the financial support by the National Science Foundation of China (No. 31601468), technological expertise and academic leaders training plan of Jiangxi Province (No. 20162BCB22009) and Key Project of Science Foundation of Jiangxi Province (No. S2017ZRZDB0192).

## References

- 1 P. Anand, A. B. Kunnumakkara, R. A. Newman and B. B. Aggarwal, *Mol. Pharm.*, 2007, **4**, 807–818.
- 2 S. Ghosh, S. Banerjee and P. C. Sil, *Food Chem. Toxicol.*, 2015, **83**, 111–124.
- 3 M. Heger, R. F. van Golen, M. Broekgaarden and M. C. Michel, *Pharmacol. Rev.*, 2014, **66**, 222–307.
- 4 L. Q. Zou, B. J. Zheng, R. J. Zhang, Z. P. Zhang, W. Liu, C. M. Liu, H. Xiao and D. J. McClements, *Food Res. Int.*, 2016, **81**, 74–82.
- 5 C. Wang, Z. Liu, G. Xu, B. Yin and P. Yao, *Food Hydrocolloids*, 2016, **61**, 11–19.
- 6 M. Massaro, R. Amaratib, G. Cavallaro, S. Guernellib, G. Lazzarac, S. Miliotoc, R. Notoa, P. Pomad and S. Riela, *Colloids Surf., B*, 2016, **140**, 505–513.
- 7 G. Cavallaro, G. Lazzara, M. Massaro, S. Milioto, R. Noto, F. Parisi and S. Riela, *J. Phys. Chem. C*, 2015, **119**, 8944–8951.
- 8 M. Massaro, S. Riela, P. Lo Meo, R. Noto, G. Cavallaro, S. Milioto and G. Lazzara, *J. Mater. Chem. B*, 2014, **2**, 7732–7738.
- 9 M. Mouslmani, J. M. Rosenholm, N. Prabhakar, M. Peurla, E. Baydoun and D. Patra, *RSC Adv.*, 2015, **5**, 18740–18750.
- 10 D. Patra and F. Sleem, *Anal. Chim. Acta*, 2013, **795**, 60–68.
- 11 L. Zou, B. Zheng, W. Liu, C. Liu, H. Xiao and D. J. McClements, *J. Funct. Foods*, 2015, **15**, 72–83.
- 12 L. Zou, W. Liu, C. Liu, H. Xiao and D. J. McClements, *J. Agric. Food Chem.*, 2015, **63**, 2052–2062.





- 13 L. Zou, B. Zheng, R. Zhang, Z. Zhang, W. Liu, C. Liu, G. Zhang, H. Xiao and D. J. McClements, *Food Biophys.*, 2016, **11**, 213–225.
- 14 X. Chen, L. Q. Zou, J. Niu, W. Liu, S. F. Peng and C. M. Liu, *Molecules*, 2015, **20**, 14293–14311.
- 15 H. H. Jin, Q. Lu and J. G. Jiang, *J. Dairy Sci.*, 2016, **99**, 1780–1790.
- 16 A. Akbarzadeh, R. Rezaei-Sadabady, S. Davaran, S. W. Joo, N. Zarghami, Y. Hanifehpour, M. Samiei, M. Kouhi and K. Nejati-Koshki, *Nanoscale Res. Lett.*, 2013, **8**, 1–9.
- 17 G. H. Shin, S. K. Chung, J. T. Kim, H. J. Joung and H. J. Park, *J. Agric. Food Chem.*, 2013, **61**, 11119–11126.
- 18 Y. Liu, D. Liu, L. Zhu, Q. Gan and X. Le, *Food Res. Int.*, 2015, **74**, 97–105.
- 19 M. Hasan, G. Ben Messaoud, F. Michaux, A. Tamayol, C. J. F. Kahn, N. Belhaj, M. Linder and E. Arab-Tehrany, *RSC Adv.*, 2016, **6**, 45290–45304.
- 20 Y. Niu, D. Ke, Q. Yang, X. Wang, Z. Chen, X. An and W. Shen, *Food Chem.*, 2012, **135**, 1377–1382.
- 21 S. Patra, E. Roy, R. Madhuri and P. K. Sharma, *RSC Adv.*, 2016, **6**, 85473–85485.
- 22 Q. Huang, L. Zhang, X. Sun, K. Zeng, J. Li and Y.-N. Liu, *RSC Adv.*, 2014, **4**, 59211–59217.
- 23 S. Peng, L. Zou, W. Liu, Z. Li, W. Liu, X. Hu, X. Chen and C. Liu, *Carbohydr. Polym.*, 2017, **156**, 322–332.
- 24 L. Zou, B. Zheng, R. Zhang, Z. Zhang, W. Liu, C. Liu, H. Xiao and D. J. McClements, *RSC Adv.*, 2016, **6**, 3126–3136.
- 25 K. Pan, Y. Luo, Y. Gan, S. J. Baek and Q. Zhong, *Soft Matter*, 2014, **10**, 6820–6830.
- 26 J. Feng, S. Wu, H. Wang and S. Liu, *J. Funct. Foods*, 2016, **27**, 55–68.
- 27 Y. Mao and D. J. McClements, *Food Funct.*, 2012, **3**, 1025–1034.
- 28 L. C. Price and R. Buescher, *J. Food Sci.*, 1997, **62**, 267–269.
- 29 M. H. Leung, H. Colangelo and T. W. Kee, *Langmuir*, 2008, **24**, 5672–5675.
- 30 J. Sabin, G. Prieto, J. M. Ruso, R. Hidalgo-Alvarez and F. Sarmiento, *Eur. Phys. J. E: Soft Matter Biol. Phys.*, 2006, **20**, 401–408.
- 31 E. D. El Khoury and D. Patra, *J. Mater. Chem. B*, 2013, **117**, 9699–9708.
- 32 J. Li, G. H. Shin, I. W. Lee, X. Chen and H. J. Park, *Food Hydrocolloids*, 2016, **56**, 41–49.
- 33 M. Takahashi, S. Uechi, K. Takara, Y. Asikin and K. Wada, *J. Agric. Food Chem.*, 2009, **57**, 9141–9146.
- 34 N. Saengkrit, S. Saesoo, W. Srinuanchai, S. Phunpee and U. R. Ruktanonchai, *Colloids Surf., B*, 2014, **114**, 349–356.
- 35 Y. P. Patil and S. Jadhav, *Chem. Phys. Lipids*, 2014, **177**, 8–18.
- 36 C. Sebaaly, H. Greige-Gerges, S. Stainmesse, H. Fessi and C. Charcosset, *Food Biosci.*, 2016, **15**, 1–10.
- 37 A. Laouini, C. Charcosset, H. Fessi, R. G. Holdich and G. T. Vladisavljevic, *Colloids Surf., B*, 2013, **112**, 272–278.
- 38 W. Liu, W. Liu, A. Ye, S. Peng, F. Wei, C. Liu and J. Han, *Food Chem.*, 2016, **196**, 396–404.
- 39 S. Garcia-Manyes, G. Oncins and F. Sanz, *Electrochim. Acta*, 2006, **51**, 5029–5036.
- 40 J. Sabin, G. Prieto, J. M. Ruso and F. Sarmiento, *Eur. Phys. J. E: Soft Matter Biol. Phys.*, 2007, **24**, 201–210.
- 41 F. Ghezzi and J. Earnshaw, *J. Phys.: Condens. Matter*, 1997, **9**, L517–L523.
- 42 A. Pérez-Lara, A. Ausili, F. J. Aranda, A. d. Godos, A. Torrecillas, S. Corbalán-García and J. C. Gómez-Fernández, *J. Phys. Chem. B*, 2010, **114**, 9778–9786.
- 43 J. Barry, M. Fritz, J. R. Brender, P. E. Smith, D. K. Lee and A. Ramamoorthy, *J. Am. Chem. Soc.*, 2009, **131**, 4490–4498.
- 44 E. Fernandez-Garcia, I. Carvajal-Lerida and A. Perez-Galvez, *Nutr. Res.*, 2009, **29**, 751–760.

